Projected major fire and vegetation changes in the Pacific Northwest of the conterminous United States under selected CMIP5 cli....

Article *in* Ecological Modelling · December 2015

DOI: 10.1016/j.ecolmodel.2015.08.023

CITATIONS
17

READS
170

3 authors:

Tim Sheehan
Conservation Biology Institute
22 PUBLICATIONS **74** CITATIONS
SEE PROFILE

Dominique Bachelet
Oregon State University
169 PUBLICATIONS **6,061** CITATIONS
SEE PROFILE

Ken Ferschweiler
Conservation Biology Institute
22 PUBLICATIONS **91** CITATIONS
SEE PROFILE

Ecological Modelling 317 (2015) 16–29

Contents lists available at ScienceDirect

Ecological Modelling

journal homepage: www.elsevier.com/locate/ecolmodel

Projected major fire and vegetation changes in the Pacific Northwest of the conterminous United States under selected CMIP5 climate futures

T. Sheehan*, D. Bachelet, K. Ferschweiler

Conservation Biology Institute, Corvallis, OR, United States

ARTICLE INFO

Article history:
Received 11 May 2015
Received in revised form 24 August 2015
Accepted 25 August 2015

Keywords:
Climate
Vegetation
Modeling
MC2
Fire
Pacific Northwest
United States
CMIP5

ABSTRACT

Climate change adaptation and mitigation require understanding of vegetation response to climate change. Using the MC2 dynamic global vegetation model (DGVM) we simulate vegetation for the Northwest United States using results from 20 different Climate Model Intercomparison Project Phase 5 (CMIP5) models downscaled using the MACA algorithm. Results were generated for representative concentration pathways (RCPs) 4.5 and 8.5 under vegetation modeling scenarios with and without fire suppression for a total of 80 model runs for future projections. For analysis, results were aggregated by three subregions: the Western Northwest (WNW), from the crest of the Cascade Mountains west; Northwest Plains and Plateau (NWPP), the non-mountainous areas east of the Cascade Mountains; and Eastern Northwest Mountains (ENWM), the mountainous areas east of the Cascade Mountains. In the WNW, mean fire interval (MFI) averaged over all climate projections decreases by up to 48%, and potential vegetation shifts from conifer to mixed forest under RCP 4.5 and 8.5 with and without fire suppression. In the NWPP MFI averaged over all climate projections decreases by up to 82% without fire suppression and increases by up to 14% with fire suppression resulting in woodier vegetation cover. In the ENWM, MFI averaged across all climate projections decreases by up to 81%, subalpine communities are lost, but conifer forests continue to dominate the subregion in the future.

1. Introduction

Effects of warming climate have already been observed in the Pacific Northwest (PNW) (e.g. Cayan et al., 2001; Mote et al., 2005), and projections indicate further warming throughout the 21st century (e.g. Mote and Salathé, 2010). In some areas, impacts of climate change may lead to widespread ecological disruption (Rehfeldt et al., 2006). Regional efforts toward climate change adaptation and mitigation require some understanding of the vegetation response to climate change (Chmura et al., 2011) and must take into account variation in projected future conditions (Millar et al., 2007).

In this context, a variety of regional studies within or including the Pacific Northwest (PNW) have examined potential climate-driven changes in the distribution of vegetation cover types and species (e.g. Rehfeldt et al., 2006; Littell et al., 2010; Rogers et al., 2011; Coops et al., 2011; Creutzburg et al., 2014; Rehfeldt et al., 2014a,b,c). Other studies have focused on the potential effects of PNW regional climate change on fire regime (Whitlock et al., 2003), insect population dynamics (Bentz et al., 2010), and forest productivity (Latta et al., 2009).

Modeling approaches have included process-based dynamic global vegetation models (DGVMs) (e.g. Rogers et al., 2011), statistical methods such as random forests classification (e.g. Rehfeldt et al., 2006, 2012, 2014a), linear mixed effects models (e.g. Rehfeldt et al., 2014b), the relationship between bioclimatic variables and species (e.g. Shafer et al., 2001), and hybrid approaches, such as combining process-based model results with statistical classification tree methods (e.g. Coops and Waring, 2011) or with state and transition models (STMs) (e.g. Creutzburg et al., 2014; Halofsky et al., 2014).

The *Integrated Scenarios of Climate, Hydrology and Vegetation* project (http://bit.ly/104rQiB) was a collaboration between the Northwest Climate Science Center, the University of Idaho, Conservation Biology Institute, and the University of Washington. The goal was to model future changes in climate, hydrology, and vegetation over the western United States from the coast to the Great Plains. Results from the Climate Model Intercomparison Project Phase 5 (CMIP5, http://cmip-pcmdi.llnl.gov/cmip5/) were

* Corresponding author at: Conservation Biology Institute, 136 SW Washington Avenue, Ste 202, Corvallis, OR 97333, United States. Tel.: +1 541 368 5810; fax: +1 541 752 0518.
E-mail address: tim@consbio.org (T. Sheehan).

http://dx.doi.org/10.1016/j.ecolmodel.2015.08.023
0304-3800/

evaluated for their ability to simulate the climate of the Northwest. The most relevant models (Vano et al., 2015) were downscaled to finer grids and used in regional hydrologic and vegetation models.

This paper presents the regional results from the vegetation modeling efforts using the downscaled CMIP5 projections in the Pacific Northwest and provides an example of the insights produced through the use of a process-based vegetation model with a large number of the most recent global climate projections. Our results suggest that fire plays a major role in shaping climate change influence on vegetation.

2. Methods

2.1. Study area

For this paper we focused on the Pacific Northwest region of the conterminous United States (north of 42° latitude and west of −111° longitude). Based on topographic and climatological characteristics, we defined three subregions (Fig. 1 and Table 1) derived from the full and partial EPA Level III Ecoregions (Omernik and Griffith, 2014) within the study area (Table 1). The Western Northwest (WNW) subregion comprises the area west of the crest of the Cascade Mountains and represents 21% of the study area. It includes the Coast Range, Klamath Mountains/California High North Coast Range, Willamette Valley, Puget Lowlands, Cascades, and North Cascades Level III Ecoregions. This subregion falls under strong coastal climatological influence with warmer minimum temperatures and much greater precipitation than the other two subregions. The Northwest Plains and Plateau (NWPP) subregion comprises 38% of the area and includes the Eastern Cascades Slopes and Foothills, Northern Basin and Range, Columbia Plateau, Snake River Plain, Northwest Great Plains, and Northwest Glaciated Plains Level III Ecoregions. This subregion is lower in elevation than the Cascades and other Northwest mountain ranges. It is drier than the other two subregions and experiences higher maximum temperatures. The remaining 41% of the area is covered by the Eastern Northwest Mountains (ENWM) comprising the mountainous regions east of the Cascades. This subregion includes the Wasatch and Uinta Mountains, Wyoming Basin, Blue Mountains, Idaho Batholith, Middle Rockies, Northern Rockies, and Canadian Rockies Level III Ecoregions. It is the coldest of the subregions and has precipitation amounts intermediate to those of the other two.

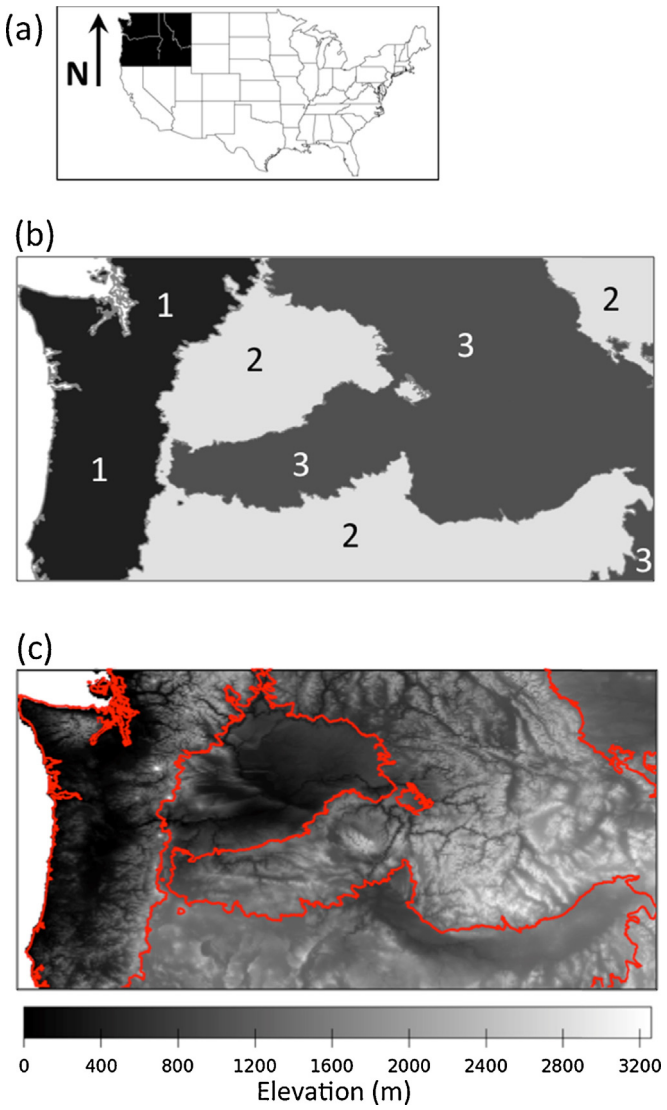

Fig. 1. (a) Index map of study area within the contiguous United States; (b) subregions defined for this study: (1) Western Northwest (WNW), (2) Northwest Plains and Plateau (NWPP), and (3) Eastern Northwest Mountains (ENWM); and (c) elevation in meters.

2.2. Model description

We used MC2, the C++ version of the MC1 dynamic global vegetation model (DGVM) (Bachelet et al., 2015). While the code structure of MC2 was modified from MC1 for purposes of performance improvement and run option specification, it uses the same algorithms as MC1 and was designed to be functionally equivalent. MC1 and MC2 have been widely used at global to regional scales to simulate potential vegetation shifts, carbon (C) fluxes, and wildfires in national parks (e.g. King et al., 2013), individual states (Lenihan et al., 2008), across the conterminous United States (Bachelet et al., 2001), North America (Drapek et al., 2015), as well as globally

Table 1
PNW subregion characteristics. Climate variables are derived from PRISM data and averaged over the historical baseline period (1971–2000).

	Area (km^2)	Mean minimum monthly temperature (°C)	Mean maximum monthly temperature (°C)	Annual precipitation (mm)	Annual summer precipitation (mm)	Level III Ecoregions
Full Study Area	784,358	0.56	13.26	842	95.76	
Western Northwest (WNW)	162,620	3.66	13.97	1841	139.95	Coast Range, Klamath Mountains/California High North Coast Range, Willamette Valley, Puget Lowlands, Cascades, North Cascades
Northwest Plains and Plateau (NWPP)	300,393	0.95	14.93	382	55.26	Eastern Cascades Slopes and Foothills, Northern Basin and Range, Columbia Plateau, Snake River Plain, Northwest Great Plains, Northwest Glaciated Plains
Eastern Northwest Mountains (ENWM)	321,345	-0.75	12.43	643	109.8	Wasatch and Uinta Mountains, Wyoming Basin, Blue Mountains, Idaho Batholith, Middle Rockies, Northern Rockies, Canadian Rockies

(Gonzalez et al., 2010) for a variety of climate change scenarios. The model is run at a monthly time step on a spatial grid in which each cell is simulated independently, with no cell-to-cell communication. The model can be used to simulate landuse (Bachelet et al., 2015), but for this project, we simulated the potential vegetation that would occur without direct human intervention. However, fire suppression and the influence of increasing atmospheric CO_2 concentrations due to anthropogenic emissions were explored in this study. The model includes three modules that simulate biogeography, biogeochemistry, and wildfire interactions.

The biogeography module simulates shifts in vegetation types based on climate and biomass thresholds. The model does not simulate individual species. Woody functional types (trees and shrubs) are distinguished by leaf phenology (evergreen vs deciduous) and morphology (needleleaf vs broadleaf). The module uses environmental gradients of minimum monthly temperature and growing season precipitation to simulate the relative dominance of woody lifeforms. The relative dominance of C3 vs C4 grasses (including forbs, sedges, and other herbaceous vegetation) is simulated by calculating the potential production of pure C3 and pure C4 stands using soil temperature. Thresholds of carbon pool values are used to distinguish between forest, savanna, shrubland, and grassland classes. There are 36 vegetation types possible, 14 of these within the temperate zone.

The model always simulates competition for light, water, and nutrients between herbaceous and woody vegetation. The biogeochemistry module is a modified version of the CENTURY model (Metherell et al., 1993) that simulates carbon and nitrogen cycles, including net primary production (plant growth) and net biological production (ecosystem carbon balance), decomposition, and soil respiration. The model simulates the allocation of carbon and nitrogen among plant parts, multiple classes of litter, and three soil organic matter pools. Woody life form and herbaceous production is limited by temperature, soil water availability, soil nitrogen, and atmospheric CO_2 (Bachelet et al., 2015). Decomposition is affected by substrate quality, soil texture and moisture, and temperature. The model also simulates actual and potential evapotranspiration (AET and PET), and soil water content in multiple soil layers. Grass and woody vegetation leaf moisture contents are calculated as functions of the ratio of available soil water to PET, and are interpreted as live fuel moisture contents affecting fire behavior.

The fire module (Lenihan et al., 1998; Conklin et al., 2015) simulates fire occurrence, area burned, and fire impacts including mortality, consumption of aboveground biomass, and nitrogen volatilization. Mortality and consumption of overstory biomass are simulated as a function of fire behavior and the canopy vertical structure. Fire occurrence is simulated as a discrete event. The module runs on a daily time step by using a randomly distributed set of daily precipitation values derived from monthly precipitation values. To estimate fuel characteristics, the module calculates the Keetch–Byram drought index (Keetch and Byram, 1968) using carbon pool values, daily precipitation, temperature, wind, potential evapotranspiration, relative humidity, and snowfall. Daily estimates for fine fuel moisture content (FFMC, Van Wagner, 1987), buildup index (BUI, Canadian Forestry Service, 1984), and energy release component (ERC, Cohen and Deeming, 1985) are also calculated. An ignition source is always assumed and a fire is simulated the first time the daily FFMC and BUI values exceed respective thresholds for current vegetation type and the fuel load is sufficiently dense to carry a fire. The model does not support more than one fire per year in a grid cell.

To reflect a realistic geographic extent of a fire under assumed ignitions, the fire module limits the area burned with an algorithm based on fire return interval (FRI) and years since last fire. In the fire module each vegetation type is assigned both a maximum and minimum FRI (Leenhouts, 1998). At each time step each grid cell's FRI is calculated starting with the maximum value for its vegetation type and adjusted as a function of BUI if the cell contains less than 70% fine fuels, or of FFMC if it contains 70% or more fine fuels. A higher BUI or FFMC reduces the FRI until it reaches the minimum FRI for that vegetation type. The maximum fraction of area burned is calculated as follows:

$$f = \frac{y}{F} \quad (1)$$

where f is the maximum fraction of area burned, y is the number of years since the last fire, and F is the fire return interval associated with the vegetation type and the severity of fuel conditions. For example, if a cell with a FRI of one hundred years had a fire five years previous, the maximum fraction of the area that could burn would be 0.05 or 5%.

The fire module includes a fire suppression option (Rogers et al., 2011) that limits the area burned to 0.06% of the cell unless the fire exceeds either an ERC of 60 or a 3.1 MW m^{-1} fireline intensity and a spread rate of 0.51 m s^{-1}. In that case, the full fire algorithm is used.

2.3. Model calibration

In vegetation modeling, it is common practice to adjust model parameters to obtain the best match possible between results using historical input data and reference datasets (benchmarks). For this study, we calibrated MC2 for the conterminous United States (CONUS) (Bachelet et al., 2015) using Kuchler's (1975) potential vegetation map, Leenhouts' (1998) potential fire return intervals matched to Kuchler's vegetation types, and the National Biomass and Carbon Dataset (NBCD) (Kellndorfer et al., 2012). Based on expert opinion, we assigned a weighted difference from 0 (full match) through 3 (full mismatch) between all possible pairs of MC2/Kuchler vegetation types. Using visual comparisons of potential vegetation departure, above ground carbon differences, and fire occurrence differences, we iteratively adjusted biogeographic parameters for vegetation type classification and BUI and FFMC thresholds for ignitions. The final parameterization produced a 47% full match (weighted difference of 0) and a 33% minimal mismatch (weighted difference of 1) between the MC2 results and Kuchler's (1975) potential vegetation, a normalized root mean square error of 0.35 for MC2 mean fire interval (MFI) vs Leenhout's (1998) FRI, and a normalized root mean square error of 0.11 vs the NBCD 2000 aboveground carbon dataset.

2.4. Run protocol

MC2 is run in three phases. In the first phase, initialization, the static biogeography model, MAPSS (Neilson, 1995) generates a map of potential vegetation distribution for the average climate between 1895 and 1924. This map is used by the biogeochemistry module to calculate initial values for carbon and nitrogen pools associated with each vegetation type with their prescribed fire return intervals. The initialization phase ends when the resistant soil carbon pool size changes by less than 1% from one year to the next. Its duration varies across the map from a few decades for grasslands up to 3000 years for temperate rainforests. Spinup, the second phase, is run iteratively using detrended historical climate from 1895 to 1924 to allow for readjustments of vegetation type and carbon pool sizes in response to interannual variability and simulated wildfires. The spinup phase ends when the net biological production (net ecosystem production minus carbon consumed by wildfire) reaches a value near zero. In the third, transient phase, the model is run with time series of historical and future climate.

2.5. Model runs

For the historical period (1895–2010) and each of the 40 climate futures (2011–2100), we ran the model once with fire suppression (FS) and once with no fire suppression (NFS). For the historical fire suppression run, fire suppression is not started until 1950 to reflect the realistic historical start of effective forest fire suppression in the United States (Pyne, 1982; Dombeck, 2001; Veblen et al., 2003). All runs used a 1/24° (~4 km) grid. The soils input dataset was originally provided by Jeff Kern for the VEMAP project (Kern, 1994, 1995, 2000), and was rescaled to match the climate grid. It includes bulk density and depth to bedrock, as well as sand, clay, and rock fragment content at three depths. Climate inputs for the historical data were upscaled to the 1/24° grid by taking the mean of 1/120° (~800 m) PRISM (Daly et al., 2008) grid cells. Projected minimum and maximum temperature, precipitation, and mean dewpoint temperature were downscaled from 40 climate futures from 20 climate models (Table 2) run for representative concentration pathways (RCPs) 4.5 and 8.5. Future climate was downscaled using the MACA algorithm (Abatzoglou and Brown, 2012), which includes steps for bias correction, epoch adjustment, and constructed analogs. All told, we executed 2 historical (FS and NFS) and 80 future runs (RCP 4.5/RCP 8.5 × FS/NFS × F 20 climate models).

2.6. Analyses

We summarized climate data and vegetation results over three thirty year periods, late 20th century (1971–2000), mid 21st century (2036–2065), and late 21st century (2071–2100). Fire results were summarized over the entire 20th and 21st centuries (1901–2000 and 2001–2100, respectively). For future projections, results were summarized by RCP/fire suppression scenario (4 separate summaries: RCP 4.5/RCP 8.5 × FS/NFS). Unless otherwise noted, for continuous output variables, summary results for future runs were produced by taking the mean over time, followed by the mean over the study area for each of the climate futures, and finally by taking the ensemble mean (mean over all climate futures) for each RCP/fire suppression scenario pair. For categorical data, we used the mode instead of the mean. Several of the climate futures used as inputs to the MC2 model runs provided data only through 2099. Ensemble results for the year 2100 were calculated considering only models for which there were data.

Climate data are summarized by subregion, and monthly precipitation is displayed by subregion. We calculated the average number of years between fires for each grid cell and called it mean fire interval (MFI) to distinguish between MC2's fire intervals and Leenhouts' FRI values used as boundaries in the fire model. At the subregional level, we calculated the maximum annual area burned

Table 2
Climate models whose results were used as inputs to MC2 for this study.

	GCM (general circulation model) or ESM (Earth System Model)	Origin	Atmosphere resolution Gridcell size (degree lat × lon) L: vertical levels
1	BCC-CSM1-1	Beijing Climate Center, China Meteorological Administration	2.8 × 2.8 L26
2	BCC-CSM1-1-M	Beijing Climate Center, China Meteorological Administration	1.12 × 1.12 L26
3	BNU-ESM	College of global change and earth system science, Beijing Normal University, China	2.8 × 1.4 L26
4	CanESM2	Canadian Center for Climate Modelling and Analysis (Canada)	2.8 × 2.8 L35
5	CCSM4	NCAR (USA)	1.25x.94 L26
6	CNRM-CM5	Meteo France and CNRS (France)	1.4 × 1.4 L31
7	CSIRO-MK3-6.0	Commonwealth Scientific and Industrial Research Organization, Queensland Climate Change Center of Excellence (Australia)	1.8 × 1.8 L18
8	GFDL-ESM2G	NOAA/GFDL (USA)	2.5 × 2.0 L48
9	GFDL-ESM2 M	NOAA/GFDL (USA)	2.5 × 2.0 L48
10	HadGEM2-CC	Meteorological Office Hadley Center, UK	1.88 × 1.25 L60
11	HadGEM2-ES	Meteorological Office Hadley Center, UK	1.88 × 1.25 L38
12	INM-CM4	Institute for Numerical Mathematics (Russia)	2.0 × 1.5 L21
13	IPSL-CM5A-LR	Institut Pierre Simon Laplace (France)	3.75 × 1.8 L39
14	IPSL-CM5A-MR	Institut Pierre Simon Laplace (France)	2.5 × 1.25 L39
15	IPSL-CM5B-LR	Institut Pierre Simon Laplace (France)	3.75 × 1.8 L39
16	MIROC5	Atmosphere and Ocean Research Institute (U. Tokyo), National Institute for Environmental Studies, Japan Agency for Marine-Earth Science and Technology (Japan)	1.4 × 1.4 L40
17	MIROC-ESM	Atmosphere and Ocean Research Institute (U. Tokyo), National Institute for Environmental Studies, Japan Agency for Marine-Earth Science and Technology (Japan)	2.8 × 2.8 L80
18	MIROC-ESM-CHEM	Atmosphere and Ocean Research Institute (U. Tokyo), National Institute for Environmental Studies, Japan Agency for Marine-Earth Science and Technology (Japan)	2.8 × 2.8 L80
19	MRI-CGCM3	Meteorological Research Institute (Japan)	1.1 × 1.1 L48
20	NorESM1-M	Norwegian Climate Center	2.5 × 1.9 L26

Table 3
MC2 vegetation types comprising this study's vegetation classes.

Vegetation class	MC2 vegetation types
Tundra	Tundra
Conifer Forest	Subalpine, Maritime Evergreen Needleleaf Forest, Temperate Evergreen Needleleaf Forest, Cool Needleleaf Forest
Cool Mixed Forest	Temperate Cool Mixed Forest
Decidous Forest	Temperate Deciduous Broadleaf Forest
Warm Mixed Forest	Temperate Warm Mixed Forest, Subtropical Mixed Forest
Woodland/Savanna	Temperate Deciduous Broadleaf Woodland, Temperate Cool Mixed Woodland, Temperate Warm Mixed Woodland, Subtropical Evergreen Broadleaf Woodland, Subtropical Mixed Woodland
Shrubland/Woodland	Temperate Evergreen Needleleaf Woodland, Temperate Shrubland, Subtropical Shrubland
Grassland	Temperate Grassland, Subtropical Grassland

and the mean annual area burned, both in terms of actual area and percent of total area. MC2 vegetation types were aggregated into broad vegetation classes to simplify the results (Table 3).

3. Results

3.1. Projected climate change

For all three regions, all climate projections show rising minimum and maximum monthly temperatures (T_{min} and T_{max}, respectively) compared to the historical baseline period (1971–2000) with ensemble mean changes ranging from 2.18 °C for mid-century average T_{min} under the RCP 4.5 scenario for WNW to 5.87 °C for late century average T_{min} under RCP 8.5 for ENWM (Table 4). Standard deviations for temperature change range from 0.54 °C (T_{min}, WNW, RCP 4.5 early century) to 1.19 °C (T_{min} and T_{max}, ENWM, RCP 8.5, late century). Temperatures rise more under RCP 8.5 than under RCP 4.5. Rising temperatures are consistent across the 21st century under RCP 8.5 while under RCP 4.5 the rate of rising slows over the later part of the century.

The change in mean annual precipitation from the late 20th century baseline is generally positive, but varies across projections (Table 4). Standard deviations range from 3.1% (Full Study Area, RCP 4.5, early century) to 7.5% (NWPP, RCP 8.5, late century). Ensemble means indicate increases for all subregion/RCP/time period combinations ranging from 0.12% (Full Study Area, RCP 4.5, early century) to 13.18% (NWPP, RCP 8.5, late century). Increases are generally largest for RCP 8.5 late century.

The change in mean summer precipitation from late 20th century is generally small but varies greatly across projections (Table 4). Standard deviations range from 8.7% (Full Study Area, RCP 8.5, early century) to 21.0% (NWPP, RCP 8.5, late century). Ensemble means indicate decreases for all subregion/RCP/time period combinations ranging from 33.14% (WNW, RCP 8.5, late century) to 13.82% (ENWM, RCP 4.5, early century). Increases are generally greatest for RCP 8.5 late century. Among all climate futures and subregions, changes ranged from −55.5% (WNW, RCP 8.5, early century) to 45.0% (NWPP, RCP 8.5, late century).

Compared to the late 20th century, summer precipitation is lower under the RCP 4.5 and 8.5 scenarios for the mid- and late 21st century, but for all climate futures the duration of the dry period is not longer (Fig. 2). During the rest of the year, especially fall (October, November, and December) and spring months (March, April, and May) precipitation generally increases (Fig. 2).

3.2. Subregional results

3.2.1. WNW

In the 21st century, the WNW subregion has a lower ensemble MFI (Table 5), a higher ensemble annual percent area burned (PAB) (Table 6), and a higher ensemble maximum annual PAB than in the 20th century across all emissions and fire suppression scenarios. Compared to results under RCP 4.5, results under RCP 8.5 show a lower MFI, larger mean annual PAB, and slightly larger maximum annual PAB. Fire suppression shows a higher MFI, lower mean PAB, and slightly lower maximum annual PAB compared to no fire suppression. During the 20th century, maximum PAB exceeds 5% one time and reaches a maximum of 10% (Fig. 3b), while during the 21st century, the ensemble mean for maximum annual PAB ranges from 13.45% (RCP 4.5 FS) to 16.96% (RCP 8.5 NFS). Results from individual future simulations range as high as 30% and encompass the 20th

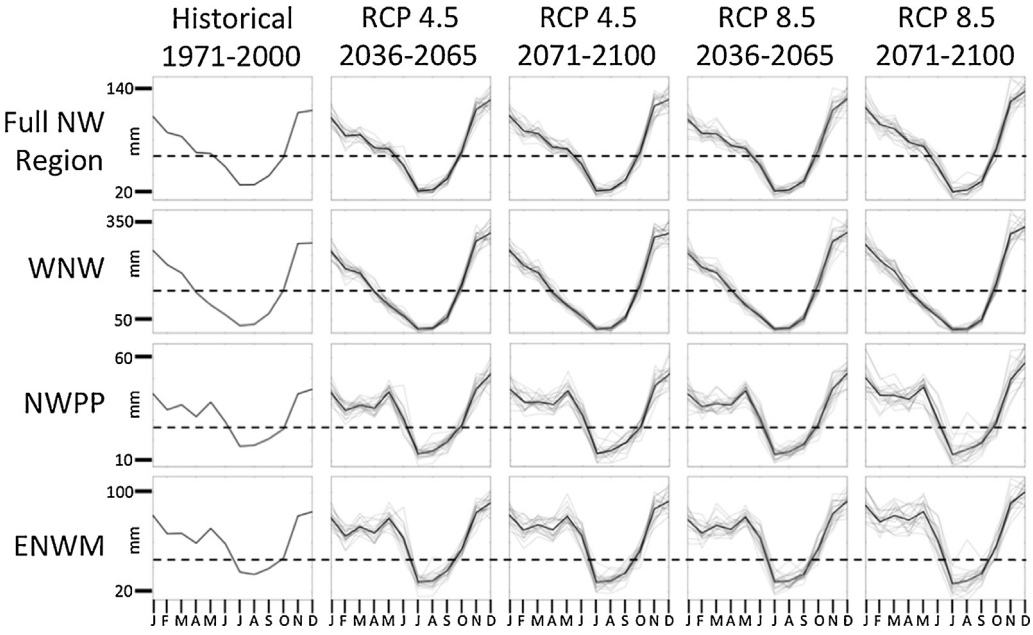

Fig. 2. Monthly precipitation by subregion, period, and representative concentration pathway (RCP). Heavy black line is ensemble mean over all climate futures, light gray lines are individual climate futures (WNW, Western Northwest; NWPP, Northwest Plains and Plateau; ENWM, Eastern Northwest Mountains).

Table 4
Changes in annual means of climate variables between historical (1971–2000) and future periods by subregion and representative concentration pathway (RCP). Ensemble means, minimums, maximums, and standard deviations were taken across results of runs produced using all climate futures.

	RCP 4.5								RCP 8.5							
	2036–2065				2071–2100				2036–2065				2071–2100			
	Min	Max	Ens. mean	SD	Min	Max	Ens. mean	SD	Min	Max	Ens. mean	SD	Min	Max	Ens. mean	SD
Full NW																
T_{min} (°C)	1.38	3.62	2.59	0.61	1.78	4.66	3.32	0.82	1.79	4.31	3.23	0.71	3.55	7.21	5.51	1.15
T_{max} (°C)	1.29	3.49	2.55	0.61	1.80	4.64	3.34	0.83	1.73	4.10	3.17	0.72	3.51	7.23	5.55	1.13
Annual ppt (% change)	−2.13	8.25	1.76	3.11	−4.61	8.98	3.39	3.84	−5.74	7.84	2.22	3.76	0.54	18.22	8.46	4.66
Summer ppt (% change)	−38.97	−1.10	−17.63	8.91	−42.66	−4.83	−18.47	9.62	−36.02	−4.73	−20.36	8.70	−48.30	15.35	−21.81	13.93
WNW																
T_{min} (°C)	1.01	2.91	2.18	0.54	1.39	3.84	2.86	0.72	1.55	3.70	2.74	0.66	2.89	6.14	4.76	1.07
T_{max} (°C)	1.05	2.94	2.21	0.54	1.66	4.10	2.93	0.70	1.56	3.68	2.77	0.64	3.09	6.24	4.84	1.01
Annual ppt (% change)	−8.14	6.60	0.12	3.69	−4.55	7.01	1.17	3.38	−9.44	8.14	0.34	4.09	−3.00	11.53	4.77	3.80
Summer ppt (% change)	−38.34	−0.75	−25.14	10.08	−43.84	−4.90	−24.66	10.44	−55.45	−14.67	−27.90	11.50	−50.76	−14.97	−33.14	10.57
NWPP																
T_{min} (°C)	1.33	3.64	2.59	0.63	1.74	4.74	3.33	0.84	1.72	4.23	3.24	0.73	3.53	7.34	5.57	1.18
T_{max} (°C)	1.34	3.69	2.61	0.65	1.92	4.92	3.43	0.88	1.73	4.28	3.25	0.75	3.61	7.65	5.71	1.17
Annual ppt (% change)	−2.61	11.30	3.67	3.63	−3.35	13.78	5.88	5.54	−5.23	12.85	4.61	4.27	1.83	27.91	13.18	7.52
Summer ppt (% change)	−40.81	9.81	−14.54	11.09	−47.50	6.30	−15.32	12.60	−30.23	0.53	−17.46	8.82	−49.85	45.02	−14.50	20.99
ENWM																
T_{min} (°C)	1.58	3.98	2.81	0.66	2.03	5.05	3.57	0.87	2.00	4.71	3.50	0.75	3.75	7.67	5.87	1.19
T_{max} (°C)	1.36	3.61	2.68	0.64	1.78	4.87	3.48	0.88	1.81	4.27	3.32	0.76	3.61	7.51	5.78	1.19
Annual ppt (% change)	−2.08	10.84	3.29	4.07	−5.42	12.24	5.44	4.89	−4.49	11.80	3.86	4.34	2.63	24.88	11.43	6.33
Summer ppt (% change)	−39.87	10.41	−13.82	10.46	−42.70	8.58	−15.61	11.52	−28.96	6.09	−16.45	10.52	−45.83	37.44	−17.34	18.08

RCP, representative concentration pathway; NW, Northwest; WNW, Western Northwest; NWPP, Northwest Plains and Plateau; ENWM, Eastern Northwest Mountains; T_{min}, minimum monthly temperature; T_{max}, maximum monthly temperature; annual ppt, full year precipitation; summer ppt, precipitation total for July–September; min, minimum from the climate futures; max: maximum from the climate futures; Ens mean: mean over climate futures; SD, standard deviation over climate futures.

Table 5
Simulated mean fire interval (MFI) by subregion for 20th century and 21st century by representative concentration pathway (RCP). Ensemble means and standard deviations were taken across results of runs produced using all climate futures.

Region and fire suppression	20th century	RCP 4.5 21st century		RCP 8.5 21st century	
		Ensemble mean	Standard deviation	Ensemble mean	Standard deviation
Full NW FS	42.36	25.87	6.72	20.81	6.69
Full NW NFS	36.66	14.60	5.65	9.35	4.99
WNW FS	81.34	47.27	11.17	37.40	10.93
WNW NFS	79.93	40.92	11.37	27.15	9.75
NWPP FS	18.56	21.10	3.77	20.01	4.70
NWPP NFS	11.39	2.84	0.98	2.05	0.69
ENWM FS	44.88	19.49	9.48	13.16	8.37
ENWM NFS	38.39	12.28	8.66	7.17	7.00

RCP, representative concentration pathway; NW, Northwest; WNW, Western Northwest; NWPP, Northwest Plains and Plateau; ENWM, Eastern Northwest Mountains; FS, fire suppression; NFS, no fire suppression.

Table 6
Simulated annual percent area burned (PAB) by subregion for 20th century and 21st century by representative concentration pathway (RCP). Ensemble means and standard deviations were taken across results of runs produced using all climate futures.

Region and fire suppression	20th century	RCP 4.5 21st century		RCP 8.5 21st century	
		Ensemble mean	Standard deviation	Ensemble mean	Standard deviation
Full NW FS	1.99	2.31	0.20	2.36	0.22
Full NW NFS	3.06	3.85	0.23	3.91	0.22
WNW FS	0.53	1.12	0.19	1.27	0.17
WNW NFS	0.58	1.32	0.23	1.52	0.19
NWPP FS	2.90	2.75	0.21	2.74	0.29
NWPP NFS	4.89	5.52	0.12	5.48	0.12
ENWM FS	1.88	2.50	0.28	2.55	0.26
ENWM NFS	2.61	3.58	0.38	3.66	0.35

RCP, representative concentration pathway; NW, Northwest; WNW, Western Northwest; NWPP, Northwest Plains and Plateau; ENWM, Eastern Northwest Mountains; FS, fire suppression; NFS, no fire suppression.

century results for maximum annual PAB (Fig. 3b). All 21st century results for mean annual PAB (Fig. 3b) lie above those for the 20th century and those for MFI (Fig. 4b) lie below. During the 20th century, most of the WNW experiences no fire regardless of whether fire suppression is applied or not (Fig. 5c). Only southern portions of the northern Cascades and southern Klamath region experience years with large areas burned by wildfire. In sharp contrast, during the 21st century, most of the area experiences extensive wildfires with PAB approaching 100% in burned grid cells, the exceptions being the Klamath area, along the Pacific coastline, and at high elevations (Fig. 5c).

Vegetation shifts from predominantly conifer to mixed forests as temperatures warm during the 21st century (Fig. 6 and Table 8). The shift starts in the south, expands along the coast, and spreads northward and upslope over the Coast Range and into the middle reaches of the Cascades. This shift is earlier and more extensive under the warmer RCP 8.5 scenario than under the cooler RCP 4.5 scenario. In the late 21st century under RCP 8.5, remnant conifer forests occur only in the northern Oregon Coast Range, the higher elevations of the Olympic Peninsula, and the higher elevations of the Cascades. Following the shift from conifer to mixed vegetation, warm mixed forests replace cool mixed forests, starting in the southwest, spreading north along the coast, and then inland and north into the foothills of the Cascades. This trend is most extensive under the RCP 8.5 scenario in the late 21st century.

3.2.2. NWPP

In the NWPP subregion, RCP scenarios have little effect on fire results (Figs. 3 and 4, and Tables 5–7), while fire suppression has a marked effect. Even though its effect during the 20th century is limited because suppression is not applied until 1950, fire suppression produces a longer MFI (18.56 years vs 11.39 years), a lower annual mean PAB (2.90% vs 4.89%), and a lower maximum annual PAB (11.95% vs 14.18%) than no fire suppression. During the 21st century fire suppression results in a MFI up to ten times as long (~20 years vs ~2–3 years), a mean PAB half as large (~2.75% vs ~5.5%), and a maximum annual PAB of just over half as large (6.79% vs 11.50% for RCP 4.5, 5.59% vs 10.80% for RCP 8.5) as those without fire suppression.

Without fire suppression, during both historical and future periods, frequent fires reduce the dominance of woody vegetation (forests and shrubs) by 9.5–12.4% (Fig. 6 and Table 8) compared to results with fire suppression. This trend is most apparent at lower elevations in the western and southern portions of the subregion where, without fire suppression, grasslands are more extensive and shrublands less. Both with and without fire suppression, the dominance of woody vegetation increases between 4.7 and 9.1% in the future period.

3.2.3. ENWM

Over the entire ENWM subregion, MFI (7.2–19.5 years 21st century vs 38.4–44.9 years 20th century) decreases, mean annual PAB (2.7–3.7% 21st century vs 1.9–2.6% 20th century) increases, and maximum annual PAB (13.5–19.4% 21st century vs 14.3–20.7% 20th century) is nearly unchanged during the 21st century as compared to the 20th century (Tables 5–7, and Figs. 3 and 4). MFI is lower, mean annual PAB higher, and maximum annual PAB higher without fire suppression. Results differ little between RCP 4.5 and 8.5 scenarios. Lower elevation valleys and slopes within the ENWM (Fig. 5) show similar responses to emission scenarios and fire suppression to comparable areas in the NWPP.

Fire in the Blue Mountains (area of generally lower elevation stretching westward from the southern portion of the subregion) differs from that in the eastern portion of the subregion, with generally more frequent, smaller fires (Fig. 5a and b) resulting in a mean annual PAB similar to that of the rest of the subregion. Fire suppression effects are consistent with those across the ENWM subregion, reducing both mean annual and maximum annual PAB,

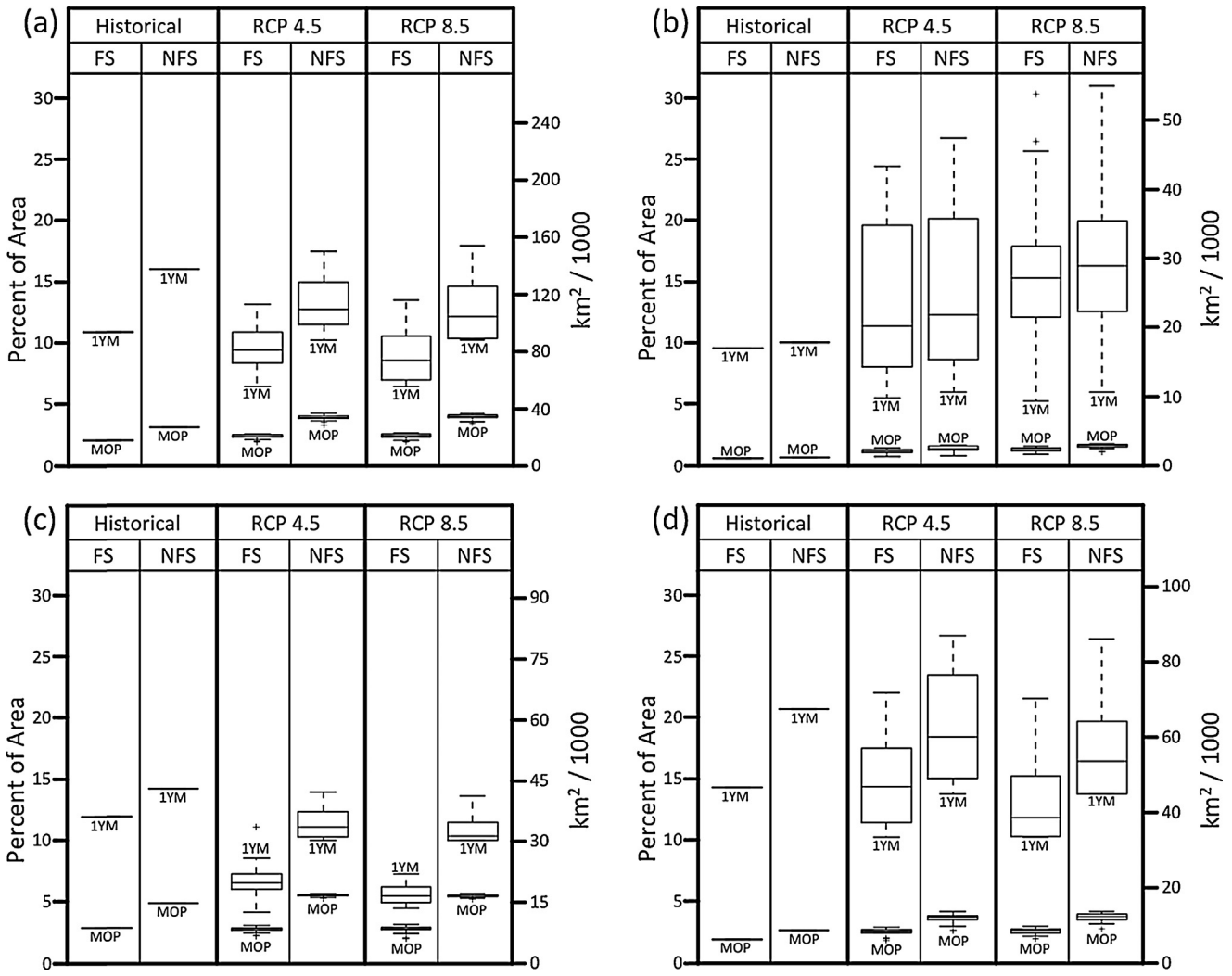

Fig. 3. Spread across model runs for mean annual area burned over time period (MOP) and maximum annual area burned (1YM) for 20th century and 21st century for two representative concentration pathways (RCPs): (a) Full Study Area, (b) WNW (Western Northwest), (c) NWPP (Northwest Plains and Plateau), and (d) ENWM (Eastern Northwest Mountains). Whiskers extend to a maximum of 1.5× interquartile range (Q3–Q1) (FS, fire suppression; NFS, no fire suppression).

and increasing MFI. In the 21st century fires are somewhat more frequent and have a somewhat higher mean annual and maximum annual PAB than those in the rest of the ENWM.

The eastern portion of the ENWM subregion exhibits different fire responses based on elevation (Fig. 5). Higher elevations have a higher MFI, lower mean annual PAB, and lower maximum annual PAB during the 20th century than lower elevations. During the 21st century, MFI decreases across this part of the subregion. Lower elevations have a higher MFI and a higher maximum annual PAB than higher elevations, but mean annual PAB similar to that of the rest of the subregion.

Conifer forests dominate the subregion for all historical and future simulations (Table 8 and Fig. 6). Conifer dominance is greater with fire suppression than without and under RCP 8.5 vs RCP 4.5. It increases through time for all future simulations. During the late 20th century, with and without fire suppression,

Table 7
Simulated maximum single year percent area burned (PAB) by subregion for 20th century and 21st century by representative concentration pathway (RCP). Ensemble means and standard deviations were taken across results of runs produced using all climate futures.

Region and fire suppression	20th century	RCP 4.5 21st century		RCP 8.5 21st century	
		Ensemble mean	Standard deviation	Ensemble mean	Standard deviation
Full NW FS	10.85	9.47	1.70	8.98	2.06
Full NW NFS	15.97	13.25	2.24	12.66	2.43
WNW FS	9.55	13.45	6.33	15.93	6.38
WNW NFS	9.97	14.20	6.60	16.96	6.79
NWPP FS	11.95	6.79	1.39	5.59	0.76
NWPP NFS	14.18	11.50	1.40	10.80	0.97
ENWM FS	14.29	14.82	3.79	13.52	3.64
ENWM NFS	20.69	19.43	4.65	17.88	4.58

RCP, representative concentration pathway; NW, Northwest; WNW, Western Northwest; NWPP, Northwest Plains and Plateau; ENWM, Eastern Northwest Mountains; FS, fire suppression; NFS, no fire suppression.

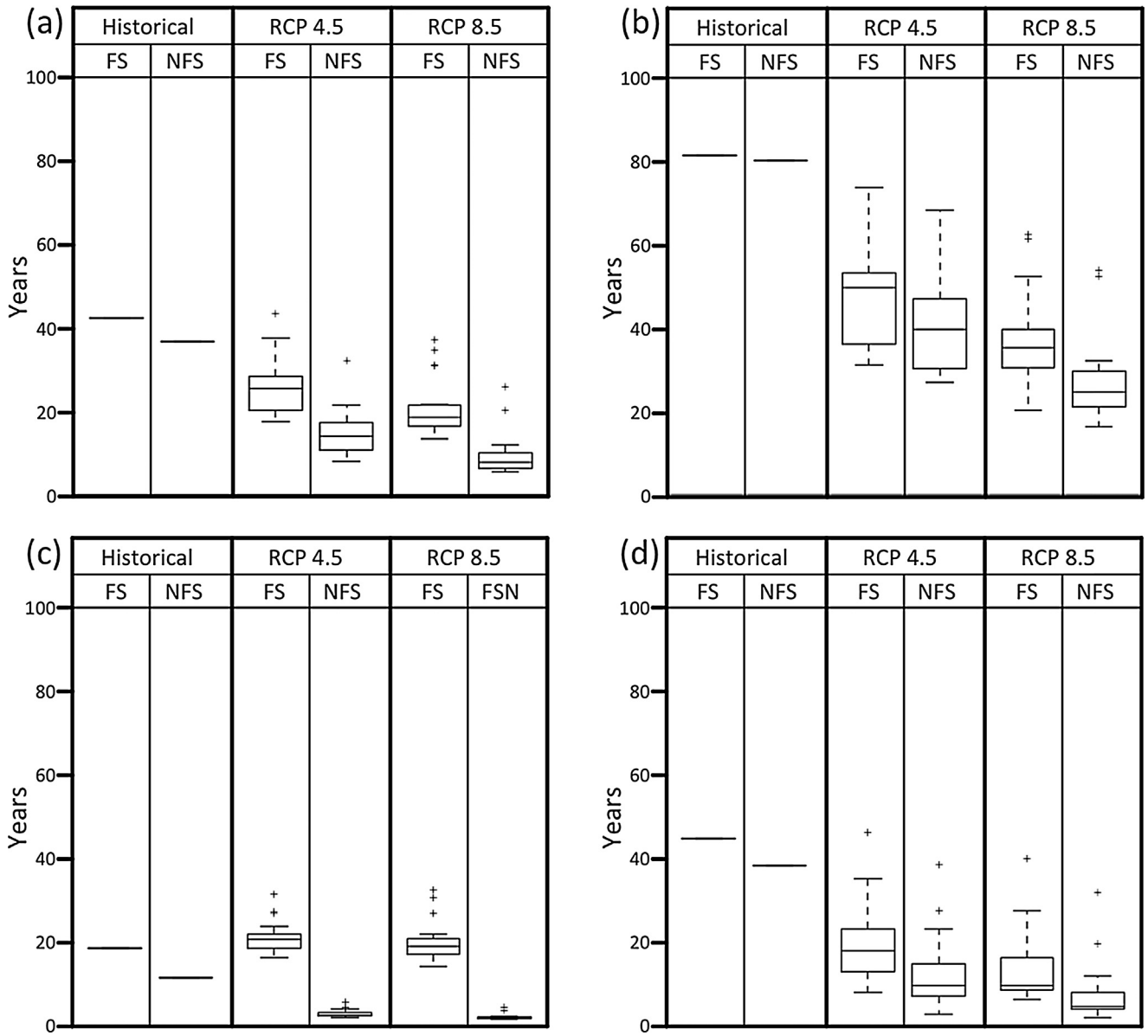

Fig. 4. Spread across model runs for simulated mean fire interval (MFI) for 20th century (Historical) and 21st century for two representative concentration pathways (RCPs): (a) Full Study Area, (b) WNW (Western Northwest), (c) NWPP (Northwest Plains and Plateau), and (d) ENWM (Eastern Northwest Mountains). Whiskers extend to a maximum of 1.5× interquartile range (Q3–Q1) (FS, fire suppression; NFS, no fire suppression).

subalpine vegetation (not shown here, part of the conifer forest vegetation type) is present at high elevation and comprises 30% of the subregion area. By the late 21st century it is nearly absent, comprising 2% and 0.3% of the subregion area for RCP 4.5 and RCP 8.5, respectively. Other vegetation type changes are limited to shifts between more or less woody types at lower elevations with conifer forest supplanting shrubland/woodland, and shrubland/woodland supplanting grassland when fire suppression is implemented.

Table 8
Dominant simulated vegetation types and percent coverage for historical and future time periods by representative concentration pathway (RCP). Results are from modes across results of runs produced using all climate futures.

Region and fire suppression	Historical		RCP 4.5				RCP 8.5			
	1971–2000		2036–2065		2070–2100		2036–2065		2070–2100	
Full NW FS	CON	47.70	CON	49.06	CON	47.52	CON	47.55	CON	49.18
Full NW NFS	CON	46.10	CON	44.05	CON	42.96	CON	42.27	CON	44.34
WNW FS	CON	85.90	CON	71.07	MIX	49.61	MIX	60.69	MIX	64.60
WNW NFS	CON	85.42	CON	70.93	MIX	49.17	MIX	60.35	MIX	64.48
NWPP FS	FSH	89.51	FSH	97.08	FSH	98.57	FSH	97.16	FSH	98.53
NWPP NFS	FSH	80.00	FSH	84.94	FSH	87.10	FSH	84.74	FSH	88.08
ENWM FS	CON	60.50	CON	66.89	CON	70.96	CON	67.60	CON	77.18
ENWM NFS	CON	58.23	CON	58.45	CON	62.75	CON	58.72	CON	68.56

RCP, representative concentration pathway; NW, Northwest; WNW, Western Northwest; NWPP, Northwest Plains and Plateau; ENWM, Eastern Northwest Mountains; FS, fire suppression; NFS, no fire suppression; CON, conifer forest; MIX, warm mixed forest + cool mixed forest; FSH, forest + shrubs.

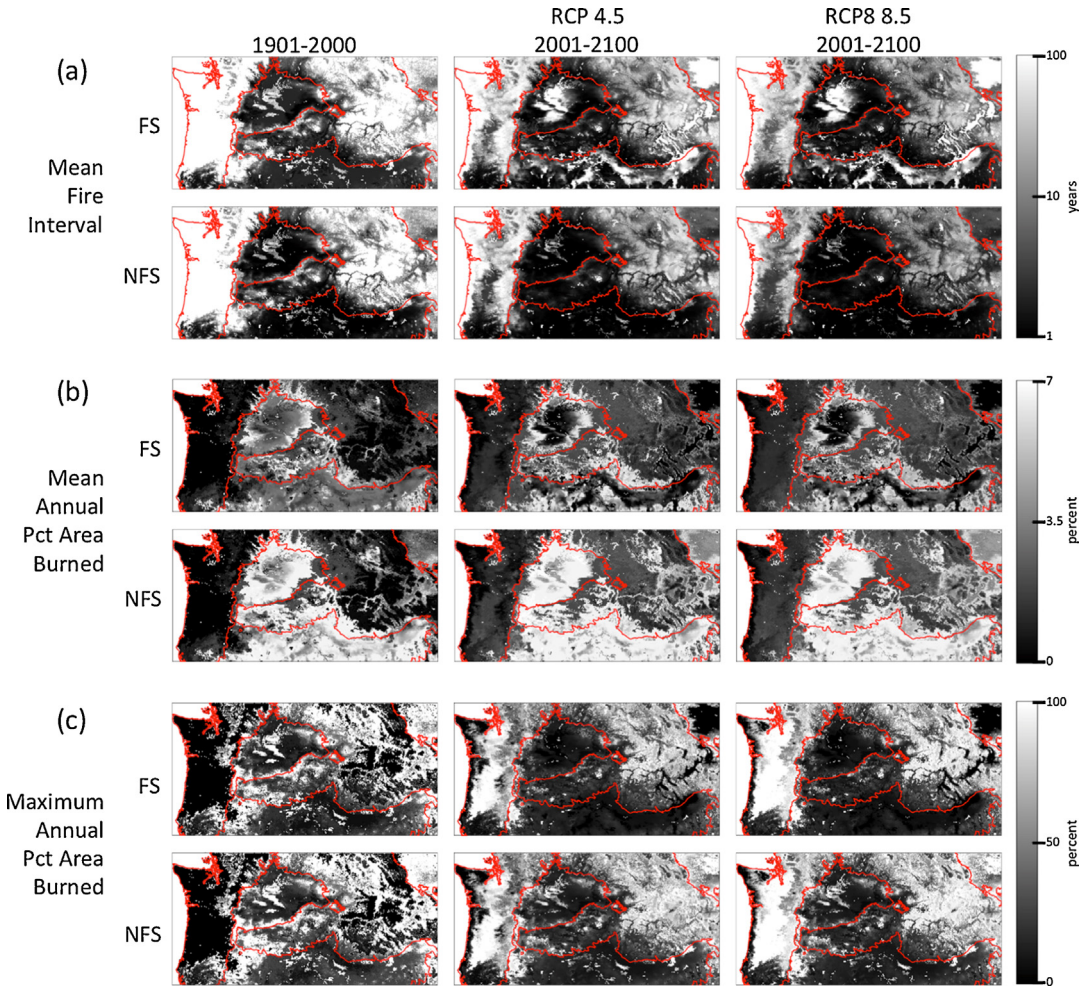

Fig. 5. Simulated fire results for 20th century and 21st century for two representative concentration pathways (RCPs) for: (a) mean fire interval (MFI), (b) mean annual percent area burned (PAB), and (c) maximum annual percent of area burned (PAB). Means and maximums taken across results of runs produced using all climate futures (Pct, percent; FS, fire suppression; NFS, no fire suppression).

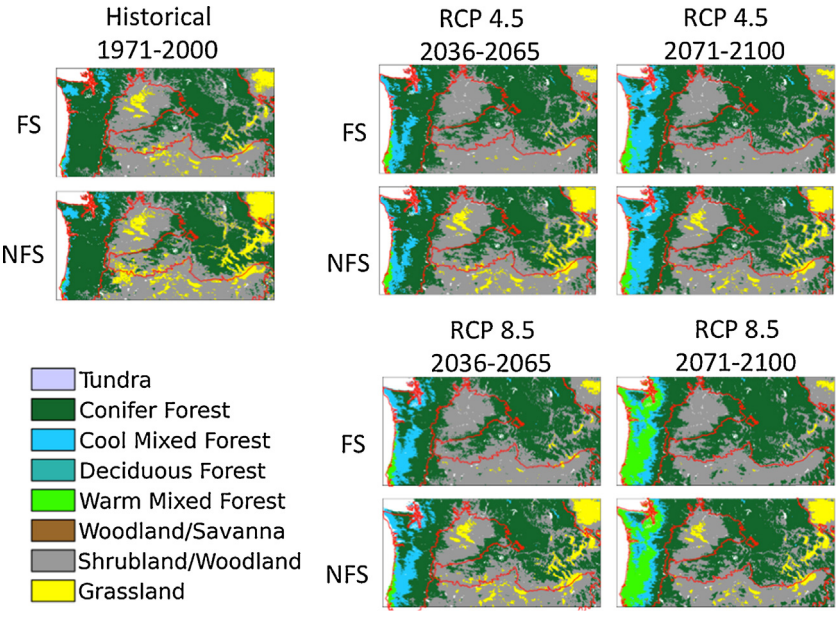

Fig. 6. Simulated modal vegetation classes for historical time period and across 20 climate futures for two representative concentration pathways (RCPs). Modes taken across results of runs produced using all climate futures (FS, fire suppression; NFS, no fire suppression).

4. Discussion

In the WNW subregion, the prevalence of large fires and the change of the dominant vegetation from conifer to mixed forest are both associated with projected increases in temperature and take place under warmer, drier summer conditions. Large fires in the WNW subregion are currently limited by fuel moisture rather than fuel amount, requiring climate conditions such as drought or extreme fire weather that have rarely occurred historically (Meyn et al., 2007). These fire-conducive conditions – warmer temperatures and drier summers – become common in the future and cause large fires. Along the trajectory from historical to future climate conditions, vegetation shifts from conifer to mixed forests are facilitated by increased wildfire occurrence in much of the subregion. However, climate, rather than fire is the driving force behind the vegetation shift. Historically droughts have led to large fires in this subregion (Agee, 1991), and the model simulated such large fires in several areas over the 20th century. In the case of either actual or simulated historical fires, conifer forests returned. Increased future temperatures and longer, dryer summers cause the vegetation to shift from the current conifer to less dense, more drought-tolerant mixed forest. This vegetation shift takes place even along the coast where moister conditions prevent fires in the future period (Fig. 6).

In MC2, the longer the period between fires, the higher the fraction of grid cell available to burn when a fire occurs. When a group of grid cells experiences a long period without burning followed by a year in which fire thresholds are exceeded, as occurs in some areas of the WNW under most climate futures, the entire area experiences a uniquely high PAB. The model is likely overestimating the annual maximum area burned in the WNW subregion. Results are best interpreted as an indication that conditions will be conducive to large fires and that if such conditions become frequent, as they are projected to under a climate with hotter, drier summers in the WNW, then large fires are likely.

In the NWPP, the use of a fixed range of FRI for each vegetation type to limit the area burned has a very strong effect on fire behavior, in turn strongly influencing the vegetation. Without fire suppression, the assumption of unlimited ignition coupled with fixed FRI leads to very frequent, small fires in grass/shrub dominated areas. This maintains grasslands by denying woody vegetation the fire-free years needed to establish. Fire suppression in the model prevents large fire occurrence even when conditions exceed fire suppression thresholds thus limiting mortality and consumption of woody vegetation and amplifying woody encroachment. The model likely overestimates fire suppression effectiveness and underestimates the frequency of shifts between grassland and shrubland with and without fire suppression. Limiting as opposed to assuming ignitions would likely lead to greater spatial variability in fire frequency, extent, and intensity. This in turn would likely result in greater spatial and temporal variation in woody vs grass vegetation dominance (Ratajczak et al., 2014).

The more frequent fire and greater mean area burned in the ENWM subregion are primarily due to rising temperatures. Although summer precipitation is reduced, the summer dry period is not longer than during the historical period (Fig. 2). Consequently the effect of the decrease in precipitation on the length of the fire season is minimal. Warmer temperatures and increased precipitation during fall, winter, and spring are not great enough to shift vegetation from conifer to mixed forest. However, along with a moderate increase in water use efficiency due to increased CO_2, these conditions result in greater conifer growth. Increased growth exceeds losses through increased fire, resulting in an overall increase in forested area. As with the WNW, assumed ignitions have led to large annual PAB in the ENWM and should be viewed in a similar manner.

Rogers et al. (2011) ran MC1 using climate data from 3 climate model projections under SRES A2 scenarios and presented results of fire suppression over the western 2/3 of the states of Oregon and Washington. For their western forest domain, which corresponds closely to our WNW subregion, the ensemble mean of their mean annual PAB (0.14%) over the historical period (1971–2000) was lower than ours over the entire 20th century (Table 6; 0.58% for NFS and 0.53% for FS). The mean of their future period (2070–2099) mean annual PAB (0.71%) was lower than ours for the 100 years of the 21st century (range of 1.12% for RCP 4.5 FS to 1.52% for RCP 8.5 NFS). From the Cascades west, their results show a similar trend with mixed forests in the Willamette Valley under the MIROC future, however they simulate a smaller extent of mixed forest in the historical and future periods than we did. Elsewhere in their study area, they generally simulated woodier vegetation than we did with more forest and less grassland and shrubland/woodland. They simulated woody vegetation increases over time, as we did with fire suppression.

More recently, using three downscaled CMIP5 climate futures representing low, moderate, and high levels of climate change, Turner et al. (2015) simulated vegetation and landuse changes in the Willamette watershed of Oregon. They found shifts in potential vegetation similar to ours for this portion of the study region, with warmer mixed forests dominating lower elevations, cooler mixed forests at intermediate elevations, and conifers remaining at high elevations. They found, as we did, that shifts to mixed and warmer mixed forest types were more extensive with the warmer drier climate scenarios. Their annual PAB for recent decades was 0.2% and they observed a 3–9-fold increase in annual area burned for their moderate to severe climate scenarios. We found that for the 20th century PAB in the WNW subregion was between 0.5% and 0.6% with a 2–3-fold increase in mean 21st century PAB. These differences are likely due to different parameterizations, since they adjusted MC2 fire thresholds for each of their runs to match local historical records, while ours was adjusted once to match CONUS reference datasets using PRISM historical data.

Differences between our results and those of Rogers et al. (2011) may be due to differences in climate futures, parameterizations, or both. Given the similarity between our results and Turner et al.'s (2015), despite independent parameterizations, it is likely that the differences are attributable to differences in the future climates used to drive the model.

West of the Cascades, Rehfeldt et al. (2006) simulated the range of Oregon coastal conifer forests shrinking to the north and west of its original range. Most of the Douglas fir forests they mapped in late 21st century were exposed to novel climate conditions. Similarly, we simulated the near complete conversion of conifer forests to mixed forests over the same region. They also mapped a larger extent of grasslands in the NWPP than we did.

Using Rehfeldt et al.'s (2006) results for Douglas fir as well as a similar, statistics-driven analysis for three pine species, Littell et al. (2010) projected Douglas-fir vulnerability and species richness gains and losses within Washington state and northern Oregon. They included vulnerability to pine beetle outbreaks (which we did not simulate) and fire in their analysis. There is general concurrence between their projections of Douglas-fir being at risk (present in <50% of models) or not at risk (present in ≥50% of models) by the 2060s and MC2 projections of conifer forests converting to mixed or remaining as conifer. However they projected unforested areas on some Cascade peaks as well as at lower elevations on the east side of Puget Sound and in lower elevation areas in the northern Willamette Valley and southern Puget Trough, while MC2 simulated forests in these areas. Overall they projected a doubling or tripling of annual area burned by the 2080s. This is lower than what MC2 simulated for the entire region, but is consistent with MC2 projections for the WNW.

Shafer et al. (2001) projected species range shifts using 3 CMIP3 futures. In the WNW, they simulated decreases in the range of Douglas-fir (*Pseudotsuga menziesii*), Pacific silver fir (*Abies amabilis*), Oregon white oak (*Quercus garryana*), and red alder (*Alnus rubra*) with increases in the ranges of valley oak (*Quercus lobata*) and ponderosa pine (*Pinus ponderosa*). This is consistent with our simulated shifts from conifer forest under cooler historical conditions to warmer mixed forests in the 21st century. They simulated the expansion of ponderosa pine within the ENWM which agrees with our simulated shifts from subalpine to warmer types at high elevations.

On a state-by-state basis for western states, McKenzie et al. (2004) used multiple regression analysis to determine the area burned as a function of summer temperature and precipitation and projected how climate change may affect area burned. Projections with the mild PCM-B2 climate projection showed increases in area burned by a factor of approximately 1.3 (Idaho) to approximately 3 (Washington) compared to the current mean. Their results are generally 20–30% greater than ours, likely as a result of their use of static vegetation while MC2 simulated shifts to more fuel-limited mixed forests over much of the study area.

Due to different modeling techniques, climate futures, and model calibrations, our results differ in specifics from those of other studies. However, they closely agree in trends toward increased fire occurrence and intensity as well as vegetation shifts. Given the uncertainties inherent in climate inputs, biogeography rules, and fire modeling, our results should be considered in the broader context of other impacts modeling work just as each general circulation model provides another projection of future climate.

5. Limitations

Climate projections generally agree on warmer future conditions, however, precipitation projections are more variable (e.g. Meehl et al., 2007). Seasonality, quantity, and interannual variability of precipitation have large effects on factors influencing fire occurrence and behavior. Years with greater precipitation can lead to increases in both dead and live fuels, in turn producing greater fire in fuel-limited areas. Dry years – or longer intraannual dry periods – can result in more fire in moisture-limited areas. Reliable soils data are key to projecting accurate soil water availability and drought stress (Peterman et al., 2014). Accurate vapor pressure deficit data are also important for producing meaningful vegetation modeling results.

MC2 simulates potential vegetation most adapted to the climate drivers. However, in reality vegetation is long lived and endures under suboptimal conditions, preventing better-suited vegetation from gaining a foothold. Vegetation can remain in a metastable state until disturbance or natural mortality removes this legacy vegetation.

Modeling fire also presents challenges as fire occurrence, spread, and intensity depend on inherently unpredictable factors including seasonal weather extremes, immediate weather conditions, ignition occurrence, and other factors that may affect fuel load and condition. A fire model will always be a simplification of dynamic processes and must strike a balance between realism, ease of implementation, and computational performance.

The effects of CO_2 concentration on water use efficiency and plant productivity are still not completely understood and may depend on factors such as ontogeny and site conditions (Camarero et al., 2015). While the CO_2 fertilization effect in MC2 is moderate, it does lead to greater woody plant production and fuel accumulation. Improved understanding of the CO_2 fertilization effects will undoubtedly lead to improvements in vegetation modeling.

The addition of insect attacks, disease, and invasive species to the model would allow the model to better reflect the effects of these influences on vegetation dynamics. However, these additions were beyond the scope of this project.

6. Conclusions

Vegetation dynamics and wildfire are inextricably linked, yet MC2 is one of the few DGVMs to include a dynamic fire model. Using MC2, we modeled future vegetation and fire for the PNW using 40 different climate futures, each with and without fire suppression. Results illustrate the range of likely future fire frequency and extent as well as the pattern of possible vegetation changes throughout the 21st century. Fire and vegetation trends were distinctly different geographically and to facilitate interpretation we summarized the results using three subregions as follows.

In the WNW, the predominant conifer forest is replaced by mixed forest under future climate scenarios. While fire is absent in most of the subregion during the 20th century, large fires are simulated during the 21st century. The metastable state of the vegetation and the potential for widespread fire indicate that this region could undergo a rapid ecological change in the coming decades. Managers will have to consider how to maintain continuity of ecosystem services and provide refugia for threatened species and communities.

Fire suppression has a significant effect in the NWPP, leading to an expansion of woody vegetation, primarily shrubs. However, the potential for periodic large fires under fire suppression is probably more likely than indicated by our results, and would likely dampen the woody expansion and possibly lead to spatial and temporal variation in grass/shrub composition. Since we do not model invasive species, their importance in changing fire regimes across the intermountain West is missing from our analysis. Managing this diverse region where invasive species and locally accumulated fuels could pose threats to existing communities presents managers with a difficult challenge.

In the ENWM, the predominant vegetation type remains conifer forest under all future climate scenarios. However, subalpine forests are supplanted by warmer forest types. The occurrence of large fires in the 21st century, especially in subalpine areas, points to the potential for sudden vegetation shifts. The possibility of rapid ecological change facilitated by sudden large fires and other disturbances is real and might affect the effectiveness of management strategies designed to maintain ecosystem resilience and future ecosystem health.

The Pacific Northwest is an ecologically diverse region that provides many ecosystem services including timber, carbon sequestration, grazing, wildlife habitat, and recreation. In addition it is home to a number of ecosystems under pressure from landuse, invasive species, and changing climate. There is little doubt that the last of these pressures will have an increasing influence as climate change effects increase into the future. Because of this, it is important that land managers – from national leaders to regional planners – utilize the best available projections for future climate, vegetation, and landuse. This study provides one example of actionable projections and provides a platform for further enhancements to best address ecological issues into the future.

Acknowledgments

Funding for this research was provided by the U.S. Department of the Interior via the Northwest Climate Science Center through agreement #G12AC20495 within the framework of the research project entitled “Integrated Scenarios of climate, hydrology and

vegetation for the Northwest", P. Mote (Oregon State University) principal investigator.

We acknowledge the World Climate Research Programme's Working Group on Coupled Modelling, which is responsible for CMIP, and we thank the climate modeling groups (listed in Table 1 of this paper) for producing and making available their model output. For CMIP, the U.S. Department of Energy's Program for Climate Model Diagnosis and Intercomparison provides coordinating support and led development of software infrastructure in partnership with the Global Organization for Earth System Science Portals.

The authors wish to acknowledge R. Nemani (NASA) for allowing them free access to the Pleiades NASA supercomputer and John Abatzoglou and Katherine Hegewisch (both of University of Idaho) for providing the downscaled CMIP5 climate data used in this study.

We thank B. Baker and A. Syphard (CBI) for useful comments on early versions of the manuscript. We also thank the manuscript reviewers who provided thoughtful comments.

References

Abatzoglou, J.T., Brown, T.J., 2012. A comparison of statistical downscaling methods suited for wildfire applications. Int. J. Climatol. 32, 772–780.

Agee JK. Fire history of Douglas-fir forests in the Pacific Northwest. In: Ruggiero LF, Aubry KB, Carey AB, and Huff MK (technical editors), Wildlife and vegetation of unmanaged Douglas-fir forests, pp. 25–33. General Technical Report PNW-GTR-285. U.S. Department of Agriculture, Forest Service, Pacific Northwest Research Station; 1991. 533 p.

Bachelet, D., Neilson, R.P., Lenihan, J.M., Drapek, R.J., 2001. Climate change effects on vegetation distribution and carbon budget in the United States. Ecosystems 4 (3), 164–185, http://dx.doi.org/10.1007/s10021-001-0002-7.

Bachelet, D., Ferschweiler, K., Sheehan, T.J., Sleeter, B., Zhu, Z., 2015. Projected carbon stocks in the conterminous US with land use and variable fire regimes. Global Change Biol., http://dx.doi.org/10.1111/gcb.13048 (in press).

Bentz, B.J., Regniere, J., Fettig, C.J., Hansen, E.M., Hayes, J.L., Hicke, J.A., et al., 2010. Climate change and bark beetles of the Western United States and Canada: direct and indirect effects. Bioscience 60 (8), 602–613, http://dx.doi.org/10.1525/bio.2010.60.8.6.

Camarero, J.J., Gazol, A., Galvan, J.D., Sanguesa-Barreda, G., Gutierrez, E., 2015. Disparate effects of global-change drivers on mountain conifer forests: warming-induced growth enhancement in young trees vs CO_2 fertilization in old trees from wet sites. Global Change Biol. 21, 738–749.

Canadian Forestry Service, 1984. Tables for the Canadian Forest Fire Weather Index System. Forestry technical report 25, 4th ed. Environment Canada, Canadian Forest Service, Ottawa, ON, pp. 48, Available at: http://www.frames.gov/documents/catalog/cfs_1984_cffdrs_fwi_tables.pdf.

Cayan, D.R., Kammerdiener, S.A., Dettinger, M.D., Caprio, J.M., Peterson, D.H., 2001. Changes in the onset of spring in the western United States. Bull. Am. Meteorol. Soc. 82 (3), 399–415.

Chmura, D.J., Anderson, P.D., Howe, G.T., Harrington, C.A., Halofsky, J.E., Peterson, D.L., et al., 2011. Forest responses to climate change in the northwestern United States: ecophysiological foundations for adaptive management. For. Ecol. Manag. 261 (7), 1121–1142, http://dx.doi.org/10.1016/j.foreco.2010.12.040.

Cohen, J.D., Deeming, J.E., 1985. The national fire danger rating system: basic equations. General technical report PSW-82. U. S. Department of Agriculture, Forest Service, Pacific Southwest Research Station, Berkeley, CA, pp. 17.

Conklin, D.R., Lenihan, J.M., Bachelet, D., Neilson, R.P., Kim, J.B., 2015. MCFire model technical description. Gen. Tech. Rep. PNW-GTR-904. U.S. Department of Agriculture, Forest Service, Pacific Northwest Research Station, Portland, OR.

Coops, N.C., Waring, R.H., 2011. Estimating the vulnerability of fifteen tree species under changing climate in Northwest North America. Ecol. Modell. 222 (13), 2119–2129, http://dx.doi.org/10.1016/j.ecolmodel.2011.03.033.

Coops, N.C., Waring, R.H., Beier, C., Roy-Jauvin, R., Wang, T.L., 2011. Modeling the occurrence of 15 coniferous tree species throughout the Pacific Northwest of North America using a hybrid approach of a generic process-based growth model and decision tree analysis. Appl. Veg. Sci. 14, 402–414.

Creutzburg, M.K., Halofsky, J.E., Halofsky, J.S., Christopher, T.A., 2014. Climate change and land management in the rangelands of central Oregon. Environ. Manag. 55, 43–55.

Daly, C., Halbleib, M., Smith, J.I., Gibson, W.P., Doggett, M.K., Taylor, G.H., et al., 2008. Physiographically sensitive mapping of climatological temperature and precipitation across the conterminous United States. Int. J. Climatol. 28 (15), 2031–2064, http://dx.doi.org/10.1002/joc.1688.

Dombeck, M., 2001. How can we reduce the fire danger in the interior West? Fire Manag. Today 61 (1), 5–13.

Drapek, R.J., Kim, J.B., Neilson, R.P., 2015. Continent-wide simulations of a dynamic global vegetation model over the United States and Canada. In: Bachelet, D., Turner, D. (Eds.), Global vegetation dynamics: concepts and applications in the MC1 model: pp. 73–90. American Geophysical Union, Washington, DC, p. 208.

Gonzalez, P., Neilson, R.P., Lenihan, J.M., Drapek, R.J., 2010. Global patterns in the vulnerability of ecosystems to vegetation shifts due to climate change. Global Ecol. Biogeogr. 19 (6), 755–768, http://dx.doi.org/10.1111/j.1466-8238.2010.00558.x.

Halofsky, J.S., Halofsky, J.E., Burcsu, T., Hemstrom, M.A., 2014. Dry forest resilience varies under simulated climate-management scenarios in a central Oregon, USA landscape. Ecol. Appl. 24, 1908–1925.

Keetch, J.J., Byram, G.M., 1968. A drought index for forest fire control. Research Paper SE-38. U. S. Department of Agriculture, Forest Service, Southeastern Forest Experiment Station, Asheville, NC, pp. 35.

Kellndorfer, J., Walker, W., LaPoint, E., Bishop, J., Cormier, T., Fiske, G., et al., 2012. NACP aboveground biomass and carbon baseline data (NBCD 2000), U.S.A., 2000. Dataset. TN Oak Ridge National Laboratory Distributed Active Archive Center, Oak Ridge, http://dx.doi.org/10.3334/ORNLDAAC/1081, Available at: http://daac.ornl.gov.

Kern, J.S., 1994. Spatial patterns of soil organic-carbon in the contiguous United-States. Soil Sci. Soc. Am. J. 58 (2), 439–455.

Kern, J.S., 1995. Geographic patterns of soil water-holding capacity in the contiguous United-States. Soil Sci. Soc. Am. J. 59 (4), 1126–1133.

Kern, J.S., 2000. Erratum for Geographic patterns of soils water-holding capacity in the contiguous United States. Soil Sci. Soc. Am. J. 64, 382.

King, D.A., Bachelet, D.M., Symstad, A.J., 2013. Climate change and fire effects on a prairie-woodland ecotone: projecting species range shifts with a dynamic global vegetation model. Ecol. Evol. 3 (15), 5076–5097, http://dx.doi.org/10.1002/ece3.877.

Kuchler, A.W., 1975. Potential natural vegetation of the conterminous United States, 2nd ed. American Geographical Society, New York, NY.

Latta, G., Temesgen, H., Barrett, T.M., 2009. Mapping and imputing potential productivity of Pacific Northwest forests using climate variables. Can. J. For. Res. 39 (6), 1197–1207, http://dx.doi.org/10.1139/x09-046.

Leenhouts, B., 1998. Assessment of biomass burning in the conterminous United States. Conserv. Ecol. 2 (1), Available at: http://www.consecol.org/vol2/iss1/art1/.

Lenihan, J.M., Daly, C., Bachelet, D., Neilson, R.P., 1998. Simulating broad-scale fire severity in a Dynamic Global Vegetation Model. Northwest Sci. 72, 91–103.

Lenihan, J.M., Bachelet, D., Neilson, R.P., Drapek, R., 2008. Response of vegetation distribution, ecosystem productivity, and fire to climate change scenarios for California. Clim. Change 87 (Suppl. 1), S215–S230.

Littell, J.S., Oneil, E.E., McKenzie, D., Hicke, J.A., Lutz, J.A., Norheim, R.A., Elsner, M.M., 2010. Forest ecosystems, disturbance, and climatic change in Washington State, USA. Clim. Change 102, 129–158.

McKenzie, D., Gedalof, Z., Peterson, D.L., Mote, P., 2004. Climatic change, wildfire, and conservation. Conserv. Biol. 18, 890–902.

Meehl, G.A., Covey, C., Delworth, T., Latif, M., McAvaney, B., Mitchell, J.F., et al., 2007. The WCRP CMIP3 multi-model dataset: a new era in climate change research. Bull. Am. Meteorol. Soc. 88, 1383–1394.

Metherell, A.K., Harding, L.A., Cole, C.V., Parton, W.J., 1993. Century soil organic matter model environment – technical documentation. Agroecosystem version 4.0. Great plains system research unit technical report No. 4. U. S. Department of Agriculture, Fort Collins, CO, pp. 245.

Meyn, A., White, P.S., Buhk, C., Jentsch, A., 2007. Environmental drivers of large, infrequent wildfires: the emerging conceptual model. Prog. Phys. Geogr. 31 (3), 287–312, http://dx.doi.org/10.1177/0309133307079365.

Millar, C.I., Stephenson, N.L., Stephens, S.L., 2007. Climate change and forests of the future: managing in the face of uncertainty. Ecol. Appl. 17, 2145–2151.

Mote, P.W., Hamlet, A.F., Clark, M.P., Lettenmaier, D.P., 2005. Declining mountain snowpack in western North America. Bull. Am. Meteorol. Soc. 86, 39–49.

Mote, P.W., Salathé, E.P., 2010. Future climate in the Pacific Northwest. Clim. Change 102, 29–50.

Neilson, R.P., 1995. A model for predicting continental-scale vegetation distribution and water-balance. Ecol. Appl. 5 (2), 362–385, http://dx.doi.org/10.2307/1942028.

Omernik, J.M., Griffith, G.E., 2014. Ecoregions of the Conterminous United States: evolution of a Hierarchical Spatial Framework. Environ. Manag. 54 (6), 1249–1266, http://dx.doi.org/10.1007/s00267-014-0364-1.

Pyne, S.J., 1982. Fire in America: a cultural history of wildland and rural fire. Princeton University Press, Princeton, NJ.

Peterman, W., Bachelet, D., Ferschweiler, K., Sheehan, T., 2014. Soil depth affects simulated carbon and water in the MC2 dynamic global vegetation model. Ecol. Modell. 294, 84–93.

Ratajczak, Z., Nippert, J.B., Briggs, J.M., Blair, J.M., 2014. Fire dynamics distinguish grasslands, shrublands and woodlands as alternative attractors in the Central Great Plains of North America. J. Ecol. 102, 1374–1385.

Rehfeldt, G.E., Crookston, N.L., Saenz-Romero, C., Campbell, E.M., 2012. North American vegetation model for land-use planning in a changing climate: a solution to large classification problems. Ecol. Appl. 22, 119–141.

Rehfeldt, G.E., Crookston, N.L., Warwell, M.V., Evans, J.S., 2006. Empirical analyses of plant–climate relationships for the western United States. Int. J. Plant Sci. 167 (6), 1123–1150, http://dx.doi.org/10.1086/507711.

Rehfeldt, G.E., Jaquish, B.C., Lopez-Upton, J., Saenz-Romero, C., St Clair, J.B., Leites, L.P., et al., 2014a. Comparative genetic responses to climate for the varieties of *Pinus ponderosa* and *Pseudotsuga menziesii*: realized climate niches. For. Ecol. Manag. 324, 126–137, http://dx.doi.org/10.1016/j.foreco.2014.02.035.

Rehfeldt, G.E., Jaquish, B.C., Lopez-Upton, J., Saenz-Romero, C., St Clair, J.B., Leites, L.P., et al., 2014b. Comparative genetic responses to climate for the varieties of *Pinus ponderosa* and *Pseudotsuga menziesii*: clines in growth potential. For. Ecol. Manag. 324, 126–137, http://dx.doi.org/10.1016/j.foreco.2014.02.041.

Rehfeldt, G.E., Jaquish, B.C., Lopez-Upton, J., Saenz-Romero, C., St Clair, J.B., Leites, L.P., et al., 2014c. Comparative genetic responses to climate for the varieties of *Pinus ponderosa* and *Pseudotsuga menziesii*: reforestation. For. Ecol. Manag. 324, 126–137, http://dx.doi.org/10.1016/j.foreco.2014.02.040.

Rogers, B.M., Neilson, R.P., Drapek, R., Lenihan, J.M., Wells, J.R., Bachelet, D., et al., 2011. Impacts of climate change on fire regimes and carbon stocks of the U.S. Pacific Northwest. J. Geophys. Res. – Biogeosci. 116, http://dx.doi.org/10.1029/2011jg001695.

Shafer, S.L., Bartlein, P.J., Thompson, R.S., 2001. Potential changes in the distributions of western North America tree and shrub taxa under future climate scenarios. Ecosystems 4, 200–215, http://dx.doi.org/10.1007/s10021-001-0004-5.

Turner, D.P., Conklin, D.R., Bolte, J.P., 2015. Projected climate change impacts on forest land cover and land use over the Willamette River Basin, Oregon USA. Clim. Change, http://dx.doi.org/10.1007/s10584-015-1465-4.

Van Wagner, C.E., 1987. Development and structure of the Canadian Forest Fire Weather Index System. Technical report 35. Petawawa National Forestry Institute, Canadian Forest Service, Chalk River, Ontario, pp. 37.

Vano, J.A., Kim, J.B., Rupp, D.E., Mote, P.W., 2015. Selecting climate change scenarios using impact-relevant sensitivities. Geophys. Res. Lett. 42, 5516–5525.

Fire and climatic change in temperate ecosystems of the western Americas Veblen, T.T., Baker, W.L., Montenegro, G., Swetnam, T.W. (Eds.), 2003. Ecological studies, 160. Springer-Verlag, New York, p. 446.

Whitlock, C., Shafer, S.L., Marlon, J., 2003. The role of climate and vegetation change in shaping past and future fire regimes in the northwestern US and the implications for ecosystem management. For. Ecol. Manag. 178 (1–2), 5–21, http://dx.doi.org/10.1016/s0378-1127(03)00051-3.